CHEMISTRY
A EUROPEAN JOURNAL

DOI: 10.1002/chem.200601735

Property Tuning in Charge-Transfer Chromophores by Systematic Modulation of the Spacer between Donor and Acceptor

Filip Bureš,[a] W. Bernd Schweizer,[a] Joshua C. May,[b] Corinne Boudon,[c] Jean-Paul Gisselbrecht,[c] Maurice Gross,[c] Ivan Biaggio,[b] and François Diederich*[a]

Abstract: A series of donor–acceptor chromophores was prepared in which the spacer separating 4-dimethylanilino (DMA) donor and $C(CN)_2$ acceptor moieties is systematically varied. All of the new push–pull systems, except **4b**, are thermally stable molecules. In series **a**, the DMA rings are directly attached to the central spacer, whereas in series **b** additional acetylene moieties are inserted. X-ray crystal structures were obtained for seven of the new, intensely colored target compounds. In series **a**, the DMA rings are sterically forced out of the mean plane of the residual π system, whereas the entire conjugated π system in series **b** is nearly planar. Support for strong donor–acceptor interactions was obtained through evaluation of the quinoid character of the DMA ring and by NMR and IR spectroscopy. The UV/Vis spectra feature bathochromically shifted, intense charge-transfer bands, with the lowest energy transitions and the smallest optical gap being measured for the two-dimensionally extended chromophores **6a** and **6b**. The redox behavior of the push–pull molecules was investigated by cyclic voltammetry (CV) and differential pulse voltammetry (DPV). In the series **1b**, **2b**, **4b**, **5b**, in which the spacer between donor and acceptor moieties is systematically enlarged, the electrochemical gap decreases steadily from 1.94 V (**1b**) to 1.53 V (**5b**). This decrease is shown to be a consequence of a reduction in the D–A conjugation with increasing spacer length. Degenerate four-wave mixing experiments reveal high third-order optical nonlinearities, pointing to potentially interesting applications of some of the new chromophores in optoelectronic devices.

Keywords: conjugation · nonlinear optics · charge transfer · donor–acceptor chromophores · electrochemistry

Introduction

Molecular and polymeric donor–acceptor (push–pull) chromophores[1] continue to attract large interest for their optoelectronic properties, in particular their high second- and third-order optical nonlinearities.[2] We reported strong intramolecular charge-transfer (CT) interactions and high third-order optical nonlinearities for three classes of small push–pull chromophores, donor–acceptor-substituted tetraethynylethenes (TEEs),[3] and, more recently, donor-substituted cyanoethynylethenes (CEEs)[4] and donor-substituted 1,1,4,4-tetracyanobuta-1,3-dienes (TCBDs).[5] Useful structure–activity relationships with predictive power were established, highlighting the dependence of third-order optical nonlinearity from the energy of the longest-wavelength CT transition and the extension of the linear donor–acceptor conjugation pathways and demonstrating the beneficial effects of low molecular symmetry, and two-dimensional donor–acceptor (D–A) conjugation.[3,4a] In particular, donor-substituted CEEs showed some of the strongest third-order nonlinear responses observed today.[4a] Optical and electrochemical band-gap tuning[4b,d,e,5a] through structural variation revealed that the position of the longest-wavelength CT absorption in the UV/Vis spectra is not a good measure for the efficiency of D–A conjugation: stronger D–A coupling

[a] Dr. F. Bureš, Dr. W. B. Schweizer, Prof. Dr. F. Diederich
Laboratorium für Organische Chemie, ETH-Zürich
Hönggerberg, HCI, 8093 Zürich (Switzerland)
Fax: (+41) 1-632-1109
E-mail: diederich@org.chem.ethz.ch

[b] J. C. May, Prof. Dr. I. Biaggio
Department of Physics and Center for Optical Technologies
Lehigh University, Bethlehem, PA 18015 (USA)

[c] Prof. C. Boudon, Dr. J.-P. Gisselbrecht, Prof. Dr. M. Gross
Laboratoire d'Electrochimie et de Chimie Physique du Corps Solide
Institut de Chimie, UMR 7177, C.N.R.S
Université Louis Pasteur, 4, rue Blaise Pascal, 67000 Strasbourg (France)

Supporting information for this article is available on the WWW under http://www.chemeurj.org/ or from the author.

leads to higher energy absorptions, whereas weaker coupling between strong donor and acceptor moieties results in lower HOMO–LUMO gaps.[1e,4b] The coupling between strong donors and acceptors, and thus the optoelectronic properties, is modulated by variation of the spacer between them.[2a,j,4b] This suggested a systematic investigation of the influence of spacers on the optoelectronic properties of small push–pull chromophores. Here we report the synthesis and properties of molecules **1**–**6** featuring different conjugated spacers between the DMA donor and the $C(CN)_2$ acceptor functions (Figure 1). With their high third-order optical nonlinearities, as revealed in preliminary measurements, and their high thermal stability, some of these compounds should become interesting chromophores for thin film formation by vapor deposition techniques and applications in optoelectronic devices.

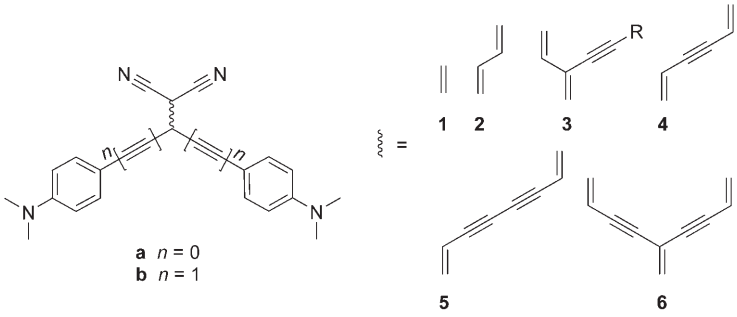

Figure 1. "Expanded" DMA-substituted cyanoethynylethenes with different spacers between donor and acceptor moieties.

Results and Discussion

Synthesis of donor–acceptor chromophores with different spacers: The preparation of compounds **1a**,[6] **1b**,[4b] and **2a**[7] has been previously described. The synthesis of **2b** started from ketone **7** (Scheme 1).[8] Deprotonation of acetaldehyde *tert*-butylimine[9] with LDA and addition to **7**, followed by imine hydrolysis, provided the unsaturated aldehyde, which was treated with malononitrile and piperidine in a Knoevenagel reaction. This sequence, however, did not provide **2b** but rather hexatriene **8**. In contrast, **2a** can be prepared in 81% yield by this route, starting from Michler's ketone. Conjugate addition of piperidine at intermediately formed **2b** under generation of **8** illustrates the strong electrophilic nature of the dicyanovinyl-activated chromophore; similar conjugate amine additions to sterically well accessible, activated alkynes had previously been observed in our laboratory.[10] When the conditions of the Knoevenagel condensation were changed, using Al_2O_3 as catalyst instead of piperidine, the desired butadiene **2b** was obtained in good yield.

On the way to chromophores **4a,b** with a central hexa-1,5-dien-3-yne-1,6-diyl spacer, the intermediate enynes **10a,b** were prepared from 3-(trimethylsilyl)propargyl alcohol by PCC oxidation[12] and Corey–Fuchs dibromoolefination[8c,13] to give **9**, followed by Suzuki cross-coupling[14] with 4-(dimethylamino)phenylboronic acid[15] or Sonogashira cross-coupling with 4-ethynyl-*N,N*-dimethylaniline (Scheme 2). Removal of the Me_3Si group in **10b** and direct lithiation was accomplished with MeLi·LiBr,[16] and reaction with DMF, followed by pouring the mixture into aqueous phosphate buffer,[17] surprisingly provided the remarkably stable aldehyde **11**, which was characterized by X-ray analysis (see Supporting Information). In contrast, enyne **10a** did not afford any aldehyde in the same transformation. Butadiene **3b** with the additional alkynyl substituent in the spacer was subsequently formed by Al_2O_3-catalyzed Knoevenagel condensation.

Removal of the Me_3Si protecting group in **10b** with nBu$_4$NF and oxidative Hay cross-coupling of the obtained terminal alkyne with propargyl alcohol afforded the moderately stable alcohol **12** (Scheme 3). Subsequent Dess–Martin oxidation[18] and Knoevenagel condensation provided **5b** with a central octa-1,7-diene-3,5-diyne-1,8-diyl spacer. While **10a** could also be deprotected, the resulting terminal alkyne did not undergo oxidative cross-coupling with propargyl alcohol, which prevented the preparation of **5a**.

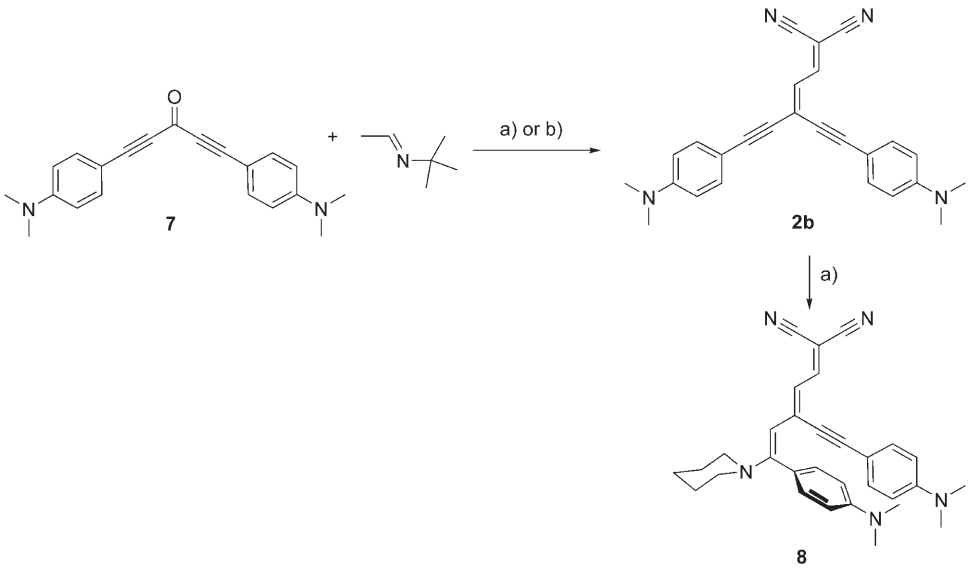

Scheme 1. Synthesis of chromophore **2b** with a central 1,3-butadiene-1,4-diyl spacer. a) 1. LDA, THF −78 °C → 20 °C, 14 h, then AcOH; 2. $(CN)_2CH_2$, piperidine, AcOH, CH_2Cl_2, 20 °C, 3 h; 37%; b) 1. LDA, THF −78 °C → 20 °C, 14 h, then aq. $ZnCl_2$; 2. $(CN)_2CH_2$, Al_2O_3 (act. II-III), CH_2Cl_2, Δ, 1 h; 71%. LDA = lithium diisopropylamide.

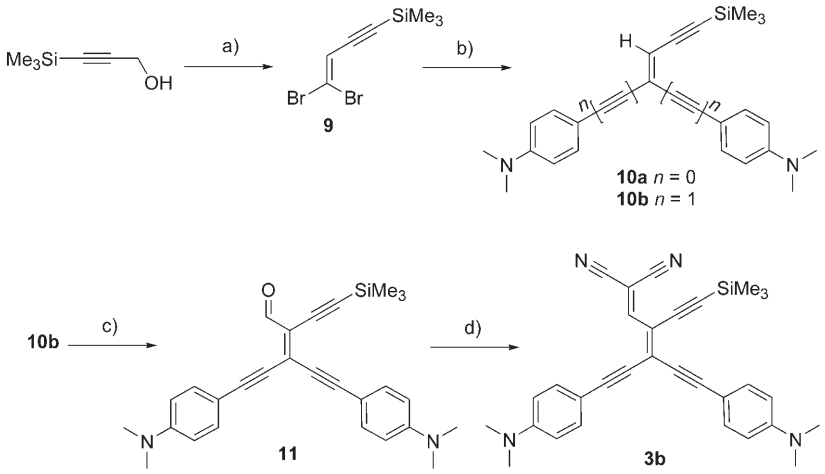

Scheme 2. Synthesis of trisalkynylated dicyanobutadiene **3b**. a) 1. PCC, Celite, mol. sieves (4) Å), CH_2Cl_2, 20 °C, 2.5 h; 2. CBr_4, PPh_3, Zn, CH_2Cl_2, 20 °C, 14 h; 69 %; b) for **10a**: 4-(dimethylamino)phenylboronic acid, $[PdCl_2(PPh_3)_2]$, Na_2CO_3, THF, H_2O, 70 °C, 14 h; 67 %; for **10b**: 4-ethynyl-*N*,*N*-dimethylaniline, $[PdCl_2(PPh_3)_2]$, CuI, Et_3N, 20 °C, 14 h; 79 %; c) MeLi.LiBr, THF, DMF, 0 °C, 1 h, then KH_2PO_4, H_2O, Et_2O, 5 °C; 67 %; d) $(CN)_2CH_2$, Al_2O_3, CH_2Cl_2, Δ, 15 min; 93 %. PCC = pyridinium chlorochromate; DMF = *N*,*N*-dimethylformamide.

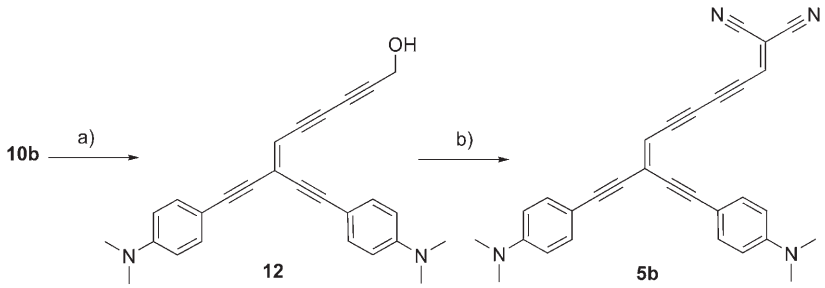

Scheme 3. Synthesis of **5b** with a central octa-3,5-diene-2,7-diyne-1,8-diyl spacer. a) nBu$_4$NF, THF, 20 °C, 1 h, then propargyl alcohol, CuCl, air, TMEDA, CH_2Cl_2, 20 °C, 14 h; 81 %; b) Dess–Martin periodinane, CH_2Cl_2, 20 °C, 1 h, then $(CN)_2CH_2$, Al_2O_3, Δ, 1 h; 87 %.

tBuMe$_2$Si-protected propargyl alcohol served as a suitable starting material for the synthesis of chromophores **4** and **6** (Scheme 4). Formylation provided aldehyde **13**, which was transformed by addition of lithiated tBuMe$_2$Si-protected propargyl alcohol and oxidation into bispropargylic ketone **14**. Dibromoolefination of **13** and **14** yielded the dibromoolefins **15** and **16**, respectively. Subsequent Suzuki or Sonogashira cross couplings led to **17a**,**b** and **18a**,**b**, respectively, from which the targeted CT chromophores **4b** and **6a**,**b** were obtained by removal of the tBuMe$_2$Si protecting groups, Dess–Martin oxidation, and Knoevenagel condensation. Target molecule **4a** could not be prepared since the alcohol, obtained by deprotection of **17a**, was found to decompose under all attempted oxidation conditions (Dess–Martin periodinane, MnO_2,[8c] PCC,[12] tetrapropylammonium perruthenate (TPAP),[19] or Swern oxidation[20]). D–A chromophore **4b** is only stable in solution; upon removal of the solvent (CH_2Cl_2), rapid decomposition to a black soot was observed.

X-ray crystal structure analysis and spectroscopic evidence for the efficiency of donor–acceptor conjugation: All target compounds, except **4b**, were obtained as stable, intensely colored solids, readily soluble in chlorinated solvents. Accordingly, crystals suitable for X-ray analysis were prepared by slow diffusion of hexane into CH_2Cl_2 solutions of the chromophore at 20 °C. The ORTEP plots in Figure 2 confirm the molecular structures assigned to **1a**, **1b**, **2a**, **2b**, **3b**, **5b**, and **6b**. The DMA moieties are roughly in plane with the residual π chromophore if separated from the central spacer by an acetylene moiety ($n = 1$, series **b**, Figure 1). In contrast, DMA rings directly attached to the central core are sterically forced out of the mean plane of the residual π chromophore ($n = 0$, series **a**) and the two aromatic rings in **1a** and **2a** adopt nonplanar conformations typical for 1,1-diarylethenes.[21] Additional crystal structures of intermediates **7** and **8** and side product **11** are reported in the Supporting Information.

Several experimental data evidencing the efficiency of ground-state CT in the new chromophores are summarized in Table 1.

The reduction in bond length alternation in the DMA rings seen in the crystal structures is a good indication for the efficiency of the intermolecular ground-state CT from the DNA donor to the cyano acceptor moieties. It can be expressed by the quinoid character (δr) of the ring according to Equation (1):

$$\delta r = [(a-b) + (c-b)]2 \approx [(a'-b') + (c'-b')]2 \quad (1)$$

where *a, b, c* and *a′, b′, c′* are the bond lengths in the DMA ring (shown for **1a** in Figure 2).[4b,22] In benzene, δr equals 0, whereas fully quinoid rings show values between 0.08 and 0.1. The data in Table 1 (δr between 0.037 and 0.070) are derived from the experimental bond lengths in the X-ray crystal structures and reveal high quinoid character for the DMA rings in the new chromophores, even exceeding previously measured values for simpler DMA-substituted CEEs and TCBDs. It should, however, be noted that the δr values bear considerable uncertainties resulting from the uncertain-

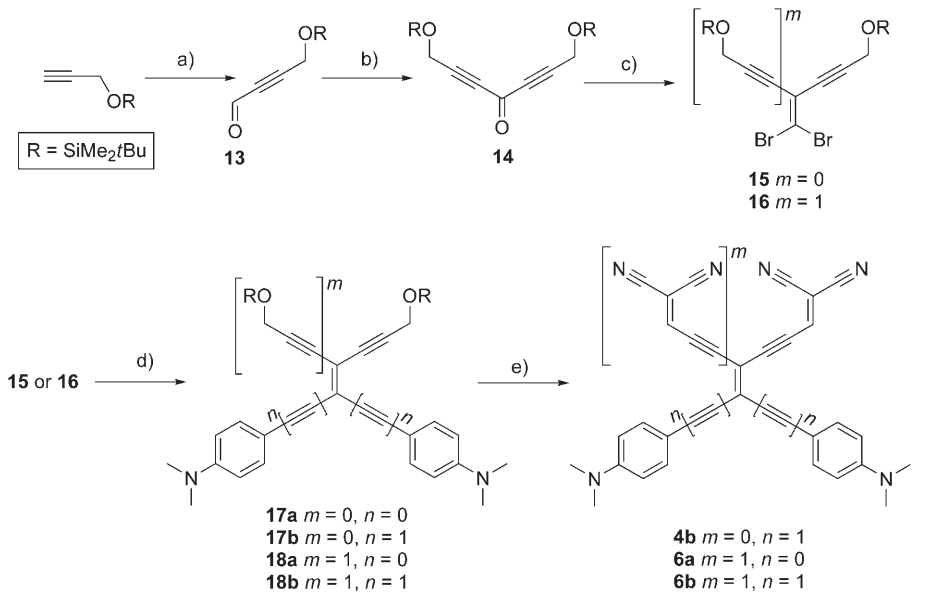

Scheme 4. Synthesis of D–A chromophores **4b** and **6a**,**b**. a) MeLi·LiBr, THF, DMF, 20 °C, 1 h, then KH_2PO_4, H_2O, Et_2O, 5 °C; 89 %; b) *t*$BuMe_2SiOCH_2$–C≡CH, *n*BuLi, THF, −20 °C, 15 min, then MnO_2, CH_2Cl_2, 20 °C, 1 h; 97 %; c) CBr_4, PPh_3, Zn, CH_2Cl_2, 20 °C, 2–24 h; 46 % (**15**), 11 % (**16**); d) for **17a**,**18a**: 4-(dimethylamino)-phenylboronic acid, $[PdCl_2(PPh_3)_2]$, Na_2CO_3, THF, H_2O, 70 °C, 14 h; 61 % (**17a**), 54 % (**18a**); for **17b**, **18b**: 4-ethynyl-*N*,*N*-dimethylaniline, $[PdCl_2(PPh_3)_2]$, CuI, Et_3N, 20 °C, 14 h; 83 % (**17b**), 74 % (**18b**); e) 1. *n*Bu_4NF, THF, 20 °C, 1 h; 2. Dess–Martin periodinane, CH_2Cl_2, 20 °C, 1 h; 3. $(CN)_2CH_2$, Al_2O_3, CH_2Cl_2, Δ, 1 h; ≈70 % (**4b**), 42 % (**6a**), 64 % (**6b**).

Table 1. Quinoid character and spectral properties evidencing the efficiency of ground-state D–A conjugation.

Compound	δr [Å][a]	δ_{meta} [ppm][b]	ν(C≡N)[cm^{-1}][c]
1a	0.046/0.070	7.37	2193
1b	[d]	7.52	2140
2a	0.067/0.037	7.35/7.11	2209
2b	[d]	7.46	2138
3b	0.069/0.064	7.47/7.44	2133
4b	[d]	7.46/7.41	[e]
5b	0.072/0.062	7.45/740	2125
6a	[f]	7.36	2145
6b	0.046/0.057	7.51	2115

[a] Quinoid character of the DMA rings (right/left according to Figure 1). [b] ^1H NMR chemical shifts ($CDCl_3$, 300 MHz) of the DMA protons *meta* to the Me_2N group. [c] Frequency of the C≡N stretch. [d] The δr values are not reliable due to disorder in the crystal structure. [e] Not determined due to instability of the solution. [f] No single crystal prepared.

ties of the individual experimental bond lengths entering Equation (1). Nevertheless, the data support strong intramolecular CT interactions in the ground state.

A comparison of the ^1H NMR chemical shifts of the DMA protons in *meta* position to the Me_2N substituent, δ_m, nicely demonstrates the beneficial contributions of the additional acetylene units in series **b** to the efficiency of ground-state CT conjugation.[4b] In the pairs of chromophores with identical central spacer (**1a**,**b**, **2a**,**b**, **6a**,**b**), this resonance appears much more downfield shifted in series **b** (Table 1), which mainly reflects a larger reduction of the electron density in the DMA rings as a result of better D–A conjugation. Most probably, the distortion of the DMA rings out of the plane of the residual π-conjugated chromophores accounts for the reduced D–A conjugation in series **a**.

The stretching frequency of the cyano groups, ν(C≡N), provides another indication for the efficiency of the intramolecular CT. This frequency shifts to lower energy when passing from series **a** to series **b** (2209 cm^{-1} (**2a**) vs. 2138 cm^{-1} (**2b**) or 2145 cm^{-1} (**6a**) vs. 2115 cm^{-1} (**6b**)), again reflecting mainly the reduced D–A conjugation in the chromophores lacking full planarity.

Electrochemistry: Electrochemical investigation of chromophores **1a–6b** carried out by cyclic voltammetry (CV) and rotating disc voltammetry (RDV) gave, for two consecutive scans, quite often irreproducible curves due to the insulating film formation either during oxidation or reduction. However, on polished electrodes, reproducible results could be observed. For these reasons, the working electrode was polished before each scan. The acquired data are summarized in Table 2. As a general trend, the first oxidation occurs on the DMA groups, whereas the first reduction involves the conjugated core bearing the cyano moieties as observed in previous studies on donor-substituted CEEs.[4b,e]

Series **a**, bearing DMA groups directly on the ethylene bridge, gave two well-separated reversible one-electron oxidations. The observed potential splitting results from electrostatic interactions occurring in the oxidized form. For chromophores **1b–6b** (series **b**), the oxidation of the DMA groups occurs in a single, irreversible two-electron step. At scan rates higher than 2 $V s^{-1}$, the electron transfer became reversible. For these compounds, no electrostatic interactions could be observed. The irreversible behavior at low scan rates denotes a lower stability of the generated bis(radical cation) than for serie **a**, presumably due to the more efficient electronic communication in the more planar chromophores.

Reduction occurs as a reversible one-electron step for chromophores **1a**, **1b**, **2a**, **2b**, and **3b**, whereas for **4b**, **5b**, **6a**, and **6b** the electron transfers were irreversible. Only the reduction of **4b** became reversible at scan rates higher than 1 $V s^{-1}$. Along the entire series (**a** and **b**), the reduction potentials were shifted to more anodic potentials, with $E_{red,1}$ in the range from −1.90 to −1.38 V for the three chromophores **1a**, **2a**, **6a** and from −1.34 to −1.00 V for chromo-

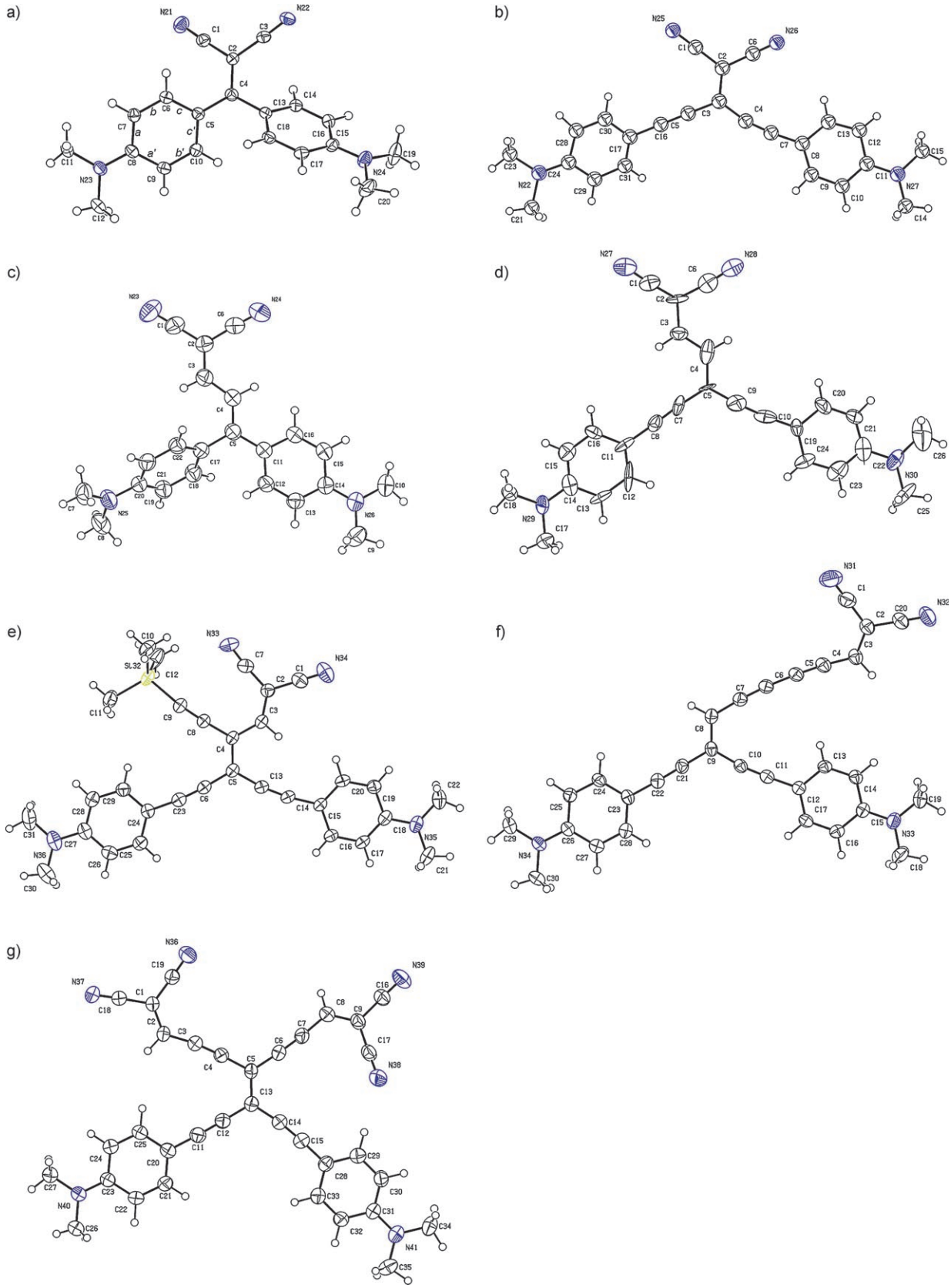

Figure 2. ORTEP representations of the new D–A chromophores a) **1a**, b) **1b**, c) **2a**, d) **2b**, e) **3b**, f) **5b**, and g) **6b** with vibrational ellipsoids obtained shown at the 50% probability level (for recording temperatures, see Supporting Information).

Table 2. Electrochemical data of chromophores **1a-6b** observed by cyclic voltammetry (CV) at a scan rate of 0.1 V s^{-1} and rotating disk voltammetry (RDV) in CH_2Cl_2 (+0.1 M nBu_4NPF_6). All potentials are given versus the ferricinium/ferrocene couple.

Compound	Cyclic voltammetry			Rotating disk voltammetry	
	$E°$ [V][a]	ΔE_p [mV][b]	E_p [V][c]	$E_{1/2}$ [V][d]	Slope [mV][e]
1a	+0.82[f]	100			
	+0.65	65		+0.65 (1e$^-$)	70
	−1.85	90		−1.90 (1e$^-$)	75
			−2.38	−2.45	75
1b			+0.75	+0.60 (2e$^-$)	[g]
	−1.27	80		−1.34 (1e$^-$)	65
			−2.06	−2.05	100
2a			+0.71[h]	+0.72 (1e$^-$)	100
	+0.51	100		+0.52 (1e$^-$)	75
	−1.61	70		−1.71 (1e$^-$)	75
			−2.28	−2.45	100
2b			+0.54	+0.53 (2e$^-$)	[g]
	−1.23	70		−1.25 (1e$^-$)	160
			−1.89	−2.07	150
3b			+0.57	+0.55 (2e$^-$)	[g]
	−1.21	90		−1.26 (1e$^-$)	90
				−1.86	100
4b			+0.43	+0.40	[g]
			−1.24	−1.18 (1e$^-$)	70
			−1.74	−1.68 (1e$^-$)	70
5b			+0.46		[g]
			−1.07	−1.06 (1e$^-$)	60
6a	+0.70	60		+0.70 (1e$^-$)	75
	+0.55	100		+0.51 (1e$^-$)	70
			−1.35	−1.38 (2e$^-$)	110
6b			+0.53	[g]	
			−0.96	−1.00	60
				−1.52	150

[a] $E° = (E_{pc} + E_{pa})/2$, where E_{pc} and E_{pa} correspond to the cathodic and anodic peak potentials, respectively. [b] $\Delta E_p = E_{ox} - E_{red}$, where the subscripts ox and red refer to the conjugated oxidation and reduction steps, respectively. [c] E_{pc} = Irreversible peak potential. [d] $E_{1/2}$ = Half-wave potential. [e] Slope of the linearized plot of E versus $\log[I/(I_{lim}-I)]$, where I_{lim} is the limiting current and I the current. [f] Reversible at scan rates >0.5 V s^{-1}. [g] Insulating film formation at the electrode surface during oxidation [h] Reversible at scan rates >1.0 V s^{-1}.

phores **1b–6b**. This reflects the reduced transfer of electron density from the DMA donor to the dicyanovinyl acceptor moieties with increasing spacer length (see below). Four cyano groups in chromophores **6a** and **6b** cause the largest anodic shift of the first reduction potential along both series ($E_{red,1} = -1.38$ V for **6a** and −1.00 V for **6b**).

UV/Vis spectroscopy: All new chromophores exhibit an intense intramolecular CT band, with the λ_{max} of compounds **1a–5b** appearing between 425 and 559 nm (Figure 3 and Figure 4, Table 2). Interestingly, the two-dimensionally conjugated chromophores **6a** and **6b** feature two particularly strongly bathochromically shifted bands at 500/632 (**6a**) and 497/629 (**6b**) nm, respectively, reflecting two different CT transitions. The CT character of the longest-wavelenth absorption of all chromophores was confirmed by protonation/neutralization experiments (see Supporting Information). Upon protonation of the Me_2N groups with *p*-toluenesulfonic acid (PTSA), all of the CH_2Cl_2 solutions turned from intensely colored (for the colors see the Supporting Information) to nearly colorless, and the longest-wavelength absorption bands disappeared almost completely. Full regeneration of the original CT band occurred upon neutralization with Et_3N (Supporting Information).

Table 3 reports both the position of the longest-wavelength CT transitions (λ_{max}) as well as the optical gaps corresponding to the end-absorption λ_{end}. Also shown are the electrochemical HOMO–LUMO gaps, calculated as the difference between first oxidation and reduction potentials $\Delta(E_{ox,1} - E_{red,1})$. A plot of the optical band gap, calculated from λ_{max} of the CT band or the end-absorption λ_{end}, for chromophores **1a**, **1b**, **2a**, **2b**, **3b**, **4b**, and **5b**, with the same number of DMA donor and CN acceptor moieties, against the electrochemical band gap shows a linear correlation ($R = 0.95$ for λ_{max} and $R = 0.97$ for λ_{end}) between the two quantities (see Supporting Information).[4b] This means that in both quantities, the same orbitals (HOMO and LUMO) are involved.

The influence of the spacer on the efficiency of the D–A conjugation is best evaluated in the series **1b**, **2b**, **4b**, **5b**, in which the donor–acceptor separation is systematically expanded. In this series, the electrochemical gap decreases steadily from 1.94 V (**1b**) to 1.53 V (**5b**) (Table 3). This decrease is a consequence of a reduction in the D–A conjugation with increasing spacer length.[4b] In DMA-substituted tetraethynylethene (TEE), the first DMA-centered oxidation occurs at +0.44 V,[23] whereas in bis-(iPr)$_3$Si-protected 1,1-dicyano-2,2-diethynylethene, the first reduction is observed at −1.15 V.[4b] The first of the two control compounds features an "unperturbed" DMA donor, the second an "unperturbed" $C(CN)_2$ acceptor. The first oxidation and reduction potentials, measured for compounds **4b** and **5b** with the larger spacers, are similar to those of the two control

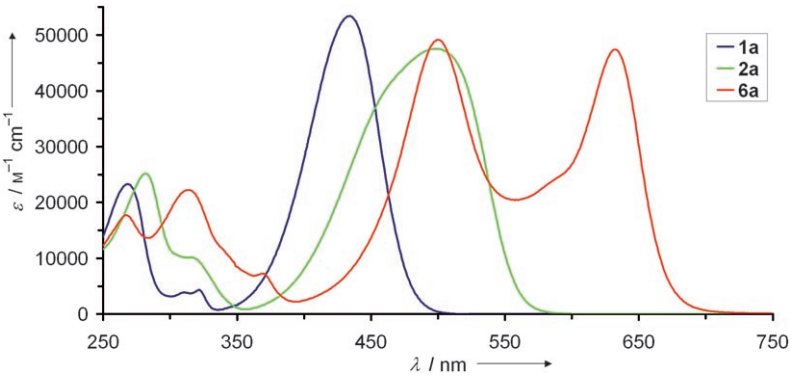

Figure 3. UV/Vis spectra of the chromophores in series **a** in CH_2Cl_2.

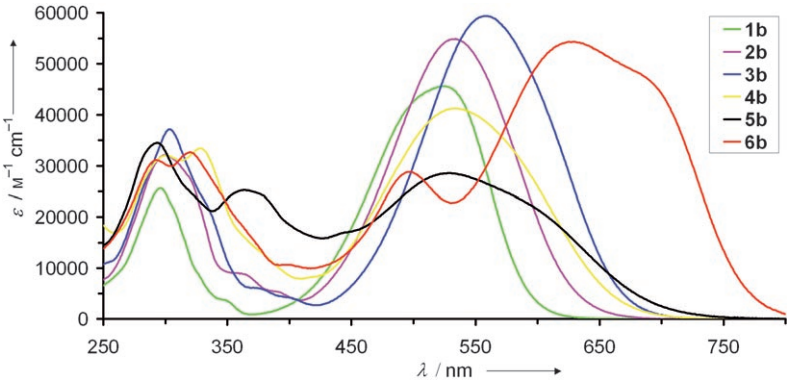

Figure 4. UV/Vis spectra of the chromophores in series **b** in CH_2Cl_2. The molar extinction coefficients of **4b** have substantial uncertainties due to the instability of the solution.

Table 3. Optical and electrochemical gaps of **1a**–**6b** determined from UV/Vis spectroscopy and CV or RDV in CH_2Cl_2.

Compound	λ_{max} [nm (eV)]	λ_{end} [nm (eV)]	$\Delta(E_{ox,1}-E_{red,1})$ [V]
1a	434 (2.88)	510 (2.43)	2.55
1b	524 (2.37	655 (1.89)	1.94
2a	498 (2.49)	590 (2.10)	2.23
2b	534 (2.32)	695 (1.78)	1.78
3b	559 (2.22)	730 (1.70)	1.81
4b	534 (2.32)[a]	740 (1.68)	1.58
5b	530 (2.34)[a]	785 (1.58)	1.53
6a	632 (1.96)	755 (1.64)	1.89
6b	629 (1.97)[a]	845 (1.47)	1.49

[a] Peak fitting by Gaussian deconvolution of the broad absorption bands of **4b**, **5b**, and **6b** gave hidden peak maxima (observed as shoulders on the broad absorptions) at $\lambda_{max}=580$ nm (2.14 eV, **4b**), 600 nm (2.07 eV, **5b**) and 700 nm (1.77 eV, **6b**).

Table 4. Third-order polarizabilities γ_{rot} measured by degenerate four-wave mixing at $\lambda=1.5$ μm in CH_2Cl_2.

Compound	$\gamma_{rot}\times10^{-48}$ m^{5}V^{-2}
1a	2 ± 2
1b	14 ± 3
2a	4 ± 3
2b	18 ± 5
3b	25 ± 3
4b	13 ± 3[a]
5b	33 ± 15
6a	8 ± 4[b]
6b	47 ± 20[b]

[a] Only stable in dichloromethane solution. [b] Low solubility in dichloromethane.

compounds in which donor and acceptor are "unperturbed" (Table 2). In contrast, in **1b** (and to a lesser extent also in **2b**), efficient D–A coupling across the shorter spacer shifts electron density from the DMA donor to the $C(CN)_2$ acceptors. As a result, the DMA-centered HOMO becomes lowered, and the $C(CN)_2$-centered LUMO is raised, leading to a larger HOMO–LUMO gap. Thus, the obtained results confirm in an impressive way previous findings that the band gap can be tuned by insertion of acetylenic and olefinic spacers that "insulate" strong donors and acceptors and reduce the efficiency of their conjugation.[4b,5a]

Nonlinear optical properties: The third-order optical nonlinearity of the new D–A chromophores was determined by measuring the third-order susceptibility of a CH_2Cl_2 solution with varying molecular concentration, which gave us the rotational average of the third-order polarizability γ_{rot}.[4a] We used degenerate four-wave mixing at a wavelength of 1.5 μm and fused silica with $\chi^{(3)}=1.9\times10^{-22}$ m^{2}V^{-2} as a reference; a detailed account of these investigations will be published elsewhere. Unless otherwise noted, the third-order polarizabilities measured in this way are off-resonant, valid in the long-wavelength limit. We found a general trend by which γ_{rot} increases with the size of the spacer between donor and acceptor groups (Table 4): The γ_{rot} obtained for chromophore **5b** was significantly larger even though its more one-dimensional geometry has a negative effect on the rotational averaging. Using chromophore **3b** as an example, we find that its rotationally averaged third-order polarizability corresponds to about 1×10^{-48} m^{5}V^{-2} for each delocalized electron (**3b** has eight double and five triple bonds), which is one measure for the efficiency of the molecular nonlinearity. Another relevant figure of merit that describes the nonlinear efficiency of a molecule is its specific third-order polarizability (γ_{rot} per molecular mass),[4a] which for this compound is 3×10^{-23} m^{5}V^{-2}Kg^{-1}. Both these values hint at a very efficient third-order nonlinearity. In fact, the third-order polarizability of **3b** is only about 50 times smaller than the fundamental maximum limit for an idealized molecule containing the same number of delocalized electrons and with the same HOMO–LUMO gap.[24] A full discussion of chromophores **6a** and **6b** is not possible at this stage because their low solubility in dichloromethane hindered a precise determination of their γ_{rot}, and because of enhancements in the experimental γ_{rot} that are caused by their 2D structure and, particularly in the case of **6b**, by the proximity of the 1.5 micrometer wavelength we used to the first two-photon absorption transition. The large off-resonant third-order polarizabilities observed in such small molecules as **2b**, **3b**, **5b** rival what was seen in the most efficient molecules measured to date.[4a] From their specific third-order polarizability one can expect that the off-resonant third-order susceptibility for a dense assembly of these molecule would be more than 3 orders of magnitude larger than for fused silica. With these nonlinear optical properties, the mentioned chromophores are attractive candidates for

device integration, in particular since many of them feature the thermal robustness required in fabrication techniques.[4a]

Conclusion

A series of new donor–acceptor chromophores was prepared in which DMA donors and $C(CN)_2$ acceptors are separated by unsaturated spacers of different size and shape. The compounds can be divided in two series: in series **a**, the DMA rings attached directly to the central spacer, whereas in series **b** they are linked through additional acetylene bridges. X-ray crystallographic analysis showed that the DMA rings in series **a** are forced out of the mean plane of the residual chromophore, whereas the entire chromophores are nearly planar in series **b**. The high quinoid character of the DMA rings in the crystal structures as well as NMR and IR data support efficient donor–acceptor conjugation in the ground state. The UV/Vis spectra of the highly colored chromophores feature intense bathochromically shifted charge-transfer bands, with two lowest-energy transitions being observed for **6a** and **6b** with multiple donor–acceptor conjugation paths. Cyclic voltammetry (CV) and differential pulse voltammetry (DPV) showed one-electron reductions centered on the DMA moieties and one-electron reductions occurring on the residual electron-accepting chromophore with the cyano moieties. This picture is in full agreement with time-dependent calculations of HOMO and LUMO in DMA-substituted cyanoethynylethenes (CEEs) such as **1b**.[4d] In the series **1b**, **2b**, **4b**, **5b**, in which the spacer between donor and acceptor moieties is systematically expanded, the electrochemical gap decreases steadily from 1.94 V (**1b**) to 1.53 V (**5b**). In agreement with previous investigations[4b,5a] this decrease is a direct consequence of a reduction in the D–A conjugation with increasing spacer length. This paper clearly demonstrates that the band gap in a series of structurally related donor–acceptor chromophores is conveniently tuned by insertion of acetylenic and/or olefinic spacers between donor and acceptor moieties. Weaker electronic donor–acceptor coupling leads to lower-energy CT absorptions and this should serve as an extremely useful guideline for chromophore design targeting optoelectronic applications. Finally, degenerate four-wave mixing experiments revealed that some of the new chromophores display very high third-order polarizabilities γ_{rot}. In view of their considerable thermal robustness, these chromophores are now investigated as components for nonlinear optics-based device fabrication.

Experimental Section

Materials and general methods: Reagents and solvents were purchased at reagent grade from Acros, Aldrich, and Fluka, and used as received. THF was freshly distilled from Na/benzophenone under N_2 atmosphere. Evaporation and concentration in vacuo was performed at water aspirator pressure. Hay catalyst refers to a freshly prepared solution of CuCl (65 mg, 0.66 mmol) and *N,N,N′,N′*-tetramethylethylenediamine (TMEDA; 80 mg, 0.69 mmol) in CH_2Cl_2 (5 mL). All reactions, except Hay couplings, were performed under an inert atmosphere by applying a positive presure of N_2. Column chromatography and plug filtrations were carried out with SiO_2 60 (particle size 0.040–0.063 mm, 230–400 mesh; Fluka) and distilled technical solvents. Thin-layer chromatography (TLC) was conducted on Al_2O_3 sheets coated with SiO_2 60 F_{254} obtained from Macherey–Nagel; visualization with a UV lamp (254 or 366 nm). Melting points (M.p.) were measured on a Büchi B-540 melting-point apparatus in open capillaries and are uncorrected. ^{1}H NMR and ^{13}C NMR spectra were measured on a Varian Gemini 300 at 20 °C. Chemical shifts are reported in ppm relative to the signal of Me_4Si. Residual solvent signals in the ^{1}H and ^{13}C NMR spectra were used as an internal reference. Coupling constants (*J*) are given in Hz. The apparent resonance multiplicity is described as s (singlet), br s (broad singlet), d (doublet), t (triplet), q (quartet), and m (multiplet). Infrared spectra (IR) were recorded on a Perkin–Elmer Spectrum BX instrument. UV/Vis spectra were recorded on a Varian Cary-5 spectrophotometer. The spectra were measured in CH_2Cl_2 in a quartz cuvette (1 cm). The absorption wavelenghts are reported in nm with the molar extinction coefficient ε (mol^{-1} dm^3cm^{-1}) in brackets; shoulders are indicated as sh. High-resolution (HR) EI-MS spectra were measured on a Hitachi-Perkin-Elmer VG-Tribrid spectrometer. HR FT-MALDI spectra were measured on an IonSpec Ultima Fourier transform (FT) instrument with [(2*E*)-3-(4-*tert*-butylphenyl)-2-methylprop-2-enylidene]malononitrile (DCTB) or 3-hydroxypicolinic acid (3-HPA) as matrix. The most important signals are reported in *m*/*z* units with *M* as the molecular ion. Elemental analyses were performed by the Mikrolabor at the Laboratorium für Organische Chemie, ETH Zürich, with a LECO CHN/900 instrument.

Acetaldehyde *tert*-butylimine was synthesized from acetaldehyde and *tert*-butylamine in 85% yield and purified by distillation (b.p. 77–80 °C) [lit.[9] b.p. 66–67 °C]. *t*$BuMe_2$Si-protected propargyl alcohol was prepared from propargyl acohol and *t*$BuMe_2SiCl$ in 93% yield following literature procedure.[25] Final purification was carried out by vacuum distillation (b. p. 27–29 °C at 0.7 Torr) [lit.[25] b.p. 48–50 at 11 Torr]. 4-(Dimethylamino)-phenylboronic acid was synthesized from 4-bromo-*N,N*-dimethylaniline following literature procedure in 61% yield.[15] 4-Ethynyl-*N,N*-dimethylaniline was prepared from 4-iodo-*N,N*-dimethylaniline and trimethylsilylacetylene by Sonogashira cross-coupling reaction and final Me_3Si group removal (K_2CO_3, MeOH) in 92% overall yield. Compounds **1a**,[6] **1b**,[4b] **2a**,[7] and **7**[8] were prepared according to literature procedure.

Electrochemistry: Electrochemical measurements were carried out in CH_2Cl_2 containing 0.1 M nBu_4NPF_6 in a classical three-electrode cell by cyclic voltammetry (CV) and rotating-disk voltammetry (RDV). The working electrode was a glassy C disk (2 mm in diameter), the auxiliary electrode a Pt wire, and the reference electrode an aqueous Ag/AgCl electrode. The cell was connected to an Autolab PGSTAT20 potentiostat (Eco Chemie, Holland) driven by a GPSE software running on a personal computer. All potentials are given versus Fc^+/Fc used as internal reference and are uncorrected from ohmic drop.

Degenerate four-wave mixing: A full account on the NLO properties of the chromophores described in this paper will be given elsewhere. For the method, see reference [4a].

X-ray analysis: CCDC-622730 (**1a**), CCDC-622731 (**1b**), CCDC-622732 (**2a**), CCDC-622733 (**2b**), CCDC-622734 (**3b**), CCDC-622735 (**5b**), CCDC-622736 (**6b**), CCDC-622737 (**7**), CCDC-622738 (**8**), and CCDC-622739 (**11**) contain the supplementary crystallographic data for this paper. These data can be obtained free of charge from The Cambridge Crystallographic Data Centre via www.ccdc.cam.ac.uk/data_request.cif.

2-{(2*Z*,4*E*)-5-[4-(Dimethylamino)phenyl]-3-[4-(dimethylamino)phenylethynyl]-5-(piperidin-1-yl)penta-2,4-dienylidene}malononitrile (8): To a stirred solution of $(iPr)_2NH$ (0.07 mL, 0.53 mmol) in THF (1 mL) at 0 °C under N_2, *n*BuLi (0.3 mL, 0.48 mmol, 1.6 M solution in hexane) was added, and the mixture stirred for 15 min. Acetaldehyde *tert*-butylimine (37.5 mg, 0.38 mmol) was added dropwise at 0 °C, and the solution was transferred to a suspension of ketone **7** (100 mg, 0.32 mmol) in THF (5 mL) at −78 °C. The mixture was allowed to reach 20 °C and stirred overnight. The orange solution was concentrated in vacuo and the residue treated (15 min) with AcOH (2 mL, 8 M solution), diluted with water

(30 mL), and extracted with Et_2O (3×50 mL). The combined organic layers were washed with saturated aqueous $NaHCO_3$ (2×50 mL), saturated aqueous NaCl, dried ($MgSO_4$), and evaporated in vacuo to leave an orange solid of crude unsaturated aldehyde. The aldehyde was taken up into CH_2Cl_2 (5 mL), and malononitrile (21 mg, 32 mmol), acetic acid (1 drop), and piperidine (1 drop) were added. The mixture was stirred for 3 h and concentrated in vacuo. Column chromatography (SiO_2; CH_2Cl_2) afforded **8** (48 mg, 37%) as a dark metallic solid. R_f=0.32 (SiO_2; CH_2Cl_2); m.p. 255–256°C; ^{1}H NMR (300 MHz, $CDCl_3$, 20°C, TMS): δ= 1.60–1.75 (m, 6H; pip.), 2.97 (s, 6H; NCH_3), 2.98 (s, 6H; NCH_3), 3.30–3.45 (m, 4H; pip.), 5.67 (s, 1H; CH), 6.40 (d, ^3J(H,H)=12.6 Hz, 1H; CH), 6.47 (d, ^3J(H,H)=9.0 Hz, 2H; Ar), 6.67 (d, ^3J(H,H)=9.0 Hz, 2H; Ar), 6.91 (d, ^3J(H,H)=8.7 Hz, 2H; Ar), 7.19 (d, ^3J(H,H)=8.7 Hz, 2H; Ar), 7.76 ppm (d, ^3J(H,H)=12.6 Hz, 1H; CH); ^{13}C NMR (75 MHz, $CDCl_3$, 20°C, TMS): δ=24.26, 26.23, 40.02, 50.89, 63.14, 77.10, 84.37, 105.45, 108.39, 110.99, 111,50, 116.19, 118.63, 119.71, 121.85, 131.71, 133.58, 144.49, 150.48, 151.97, 154.42, 164.74 ppm; IR (neat): $\tilde{\nu}$=2930, 2200, 2163, 1604, 1473, 1436, 1358, 1185, 1062, 993, 940, 873, 815, 676 cm^{-1}; UV/Vis (CH_2Cl_2): λ_{max} (ε)=290 (29500), 580 nm (sh, 59500 mol^{-1} dm^3 cm^{-1}); HR-FT-MALDI-MS (3-HPA) *m/z*: calcd for $C_{31}H_{34}N_5^+$: 476.2809; found 476.2820 ([*M*H]$^+$).

2-{5-[4-(Dimethylamino)phenyl]-3-[(4-(dimethylamino)phenylethynyl]-pent-2-en-4-ynylidene}malononitrile (2b): Into a stirred solution of (iPr)$_2$NH (0.4 mL, 3.05 mmol) in THF (5 mL) at 0°C under N_2, nBuLi (1.55 mL, 2.5 mmol, 1.6 M hexane solution) was added and the solution stirred for 15 min. Acetaldehyde *tert*-butylimine (187.5 mg, 1.9 mmol) was added dropwise at 0°C and the solution transferred to **7** (500 mg, 1.6 mmol) in THF (40 mL) at −78°C. The resulting mixture was allowed to reach 20°C and stirred overnight. The solution was concentrated in vacuo and the residue poured in a stirred solution of $ZnCl_2$ (1 g, 7.3 mmol) in water (10 mL). Et_2O (30 mL) was added and the suspension stirred for 1 h and filtered through a plug (Celite, Et_2O). The aqueous layer was extracted with Et_2O (2×25 mL), and the combined organic layers were washed with water (50 mL), dried ($MgSO_4$), and evaporated in vacuo. The residue was taken up into CH_2Cl_2 (30 mL), and malononitrile (150 mg, 2.27 mmol) followed by Al_2O_3 (600 mg, 5.9 mmol, activity II-III) were added. The mixture was heated to reflux for 1 h, filtered through a plug (SiO_2; CH_2Cl_2), and concentrated in vacuo. Column chromatography (SiO_2; CH_2Cl_2/hexane 1:1) afforded **2b** (0.44 g, 71%) as a golden metallic solid. R_f=0.6 (SiO_2; CH_2Cl_2); m.p. 245–247°C; ^{1}H NMR (300 MHz, CD_2Cl_2, 20°C, TMS): δ=3.04 (s, 6H; NCH_3), 3.05 (s, 6H; NCH_3), 6.67–6.71 (m, 4H; Ar), 7.01 (d, ^3J(H,H)=12.9 Hz, 1H; CH), 7.44–7.49 (m, 4H; Ar), 8.02 ppm (d, ^3J(H,H)=12.9 Hz, 1H; CH); ^{13}C NMR (75 MHz, CD_2Cl_2, 20°C, TMS): δ=40.03, 79.25, 85.51, 90.09, 103.41, 106.22, 106.87, 107.19, 111.81, 111.84, 112.81, 115.03, 123.65, 130.28, 134.09, 134.38, 151.77, 155.19 ppm; IR (neat): $\tilde{\nu}$=2894, 2294, 2181, 2138, 1597, 1514, 1360, 1323, 1209, 1183, 1088, 926, 860, 811, 639 cm^{-1}; UV/Vis (CH_2Cl_2): λ_{max} (ε)=299 (sh, 32000), 534 nm (55000 mol^{-1} dm^3 cm^{-1}); HR-FT-MALDI-MS (3/HPA) *m/z*: calcd for $C_{26}H_{23}N_4^+$: 391.1917; found 391.1923 ([*M*H]$^+$).

5-[4-(Dimethylamino)phenyl]-3-{[4-(dimethylamino)phenyl]ethynyl}-2-[(trimethylsilyl)ethynyl]pent-2-en-4-ynal (11): To a solution of **10b** (100 mg, 0.24 mmol) in THF (10 mL), MeLi·LiBr (0.12 mL, 0.25 mmol, 2.2 M solution in Et_2O) was added under N_2 at 0°C. The mixture turned deep red immediately and was stirred for 2 h at 0°C. DMF (0.1 mL, 1.3 mmol) was added and stirring continued for 1 h at 0°C. The mixture was poured into a vigorously stirred biphasic system of saturated aqueous KH_2PO_4 and Et_2O at 5°C (10/10 mL). The organic layer was separated and the aqueous layer extracted with Et_2O (2×20 mL). The combined organic layers were dried ($MgSO_4$), the solvents evaporated, and the residue purified by CC (SiO_2; CH_2Cl_2) to give **11** (71.7 mg, 67%) as a red solid. R_f=0.66 (SiO_2; CH_2Cl_2); m.p. >197°C (decomp); ^{1}H NMR (300 MHz, $CDCl_3$, 20°C, TMS): δ=0.30 (s, 9H; $SiCH_3$), 3.04 (s, 6H; NCH_3), 3.05 (s, 6H; NCH_3), 6.64 (d, ^3J(H,H)=9.0 Hz, 4H; Ar), 7.43 (d, ^3J(H,H)=9.0 Hz, 2H; Ar), 7.48 (d, ^3J(H,H)=9.0 Hz, 2H; Ar), 10.27 ppm (s, 1H; CHO); ^{13}C NMR (75 MHz, $CDCl_3$, 20°C, TMS): δ=−0.02, 39.97, 84.22, 88.50, 98.89, 106.19, 107.56, 107.81, 108.06, 108.81, 111.45, 111.51, 128.75, 128.01, 133.56, 134.09, 151.06, 151.14, 189.13 ppm; IR (neat): $\tilde{\nu}$= 2904, 2151, 1654, 1599, 1529, 1440, 1358, 1247, 1184, 1101, 833, 805, 752 cm^{-1}; UV/Vis (CH_2Cl_2): λ_{max} (ε)=297 (sh, 30000), 479 nm (44200 mol^{-1} dm^3 cm^{-1}); HR-FT-MALDI-MS (DCTB) *m/z*: calcd for $C_{28}H_{30}N_2OSi^+$: 438.2122; found 438.2129 ([*M*]$^+$).

2-{5-[4-(Dimethylamino)phenyl]-3-[4-(dimethylamino)phenylethynyl]-2-[(trimethylsilyl)ethynyl]pent-2-en-4-ynylidene}malononitrile (3b): To the solution of **11** (30 mg, 0.068 mmol), malononitrile (6.6 mg, 0.1 mmol) in CH_2Cl_2 (50 mL) and Al_2O_3 (50 mg, 0.5 mmol) were added and the mixture heated to reflux for 15 min. Filtration through a plug (SiO_2; CH_2Cl_2) afforded **3b** (31 mg, 93%) as a golden metallic solid. R_f=0.8 (SiO_2; CH_2Cl_2); m.p. 219–220°C; ^{1}H NMR (300 MHz, $CDCl_3$, 20°C, TMS): δ= 0.33 (s, 9H; $SiCH_3$), 3.06 (s, 6H; NCH_3), 3.07 (s, 6H, NCH_3), 6.65 (d, ^3J-(H,H)=9.0 Hz, 4H; Ar), 7.44 (d, ^3J(H,H)=9.0 Hz, 2H; Ar), 7.47 (d, ^3J-(H,H)=9.0 Hz, 2H; Ar), 7.93 ppm (s, 1H; CH); ^{13}C NMR (75 MHz, $CDCl_3$, 20°C, TMS): δ=−0.28, 40.16, 79.74, 86.59, 91.35, 96.90, 106.97, 107.73, 109.97, 110.62, 111.56, 111.62, 111.81, 112.17, 115.90, 122.16, 127.17, 133.91, 134.54, 151.36, 151.45, 152.26 ppm; IR (neat): $\tilde{\nu}$=2900, 2133, 1594, 1525, 1439, 1363, 1246, 1185, 1103, 997, 943, 841, 810, 760, 668 cm^{-1}; UV/Vis (CH_2Cl_2): λ_{max} (ε)=303 (sh, 37200), 559 nm (59400 mol^{-1} dm^3 cm^{-1}); HR-FT-MALDI-MS (DCTB) *m/z*: calcd for $C_{31}H_{30}N_4Si^+$: 486.2234; found 486.2230 ([*M*]$^+$).

"One-pot" silyl deprotection/oxidation/Knoevenagel condensation—general method: To a solution of tBuMe$_2$Si-protected alcohol (0.21 mmol) in THF (20 mL), nBu$_4$NF (0.5 mL, 0.5 mmol, 1 M THF solution) was added. The mixture was stirred for 1 h, diluted with CH_2Cl_2 (30 mL) and water (50 mL), and the layers were separated. The aqueous layer was extracted with CH_2Cl_2 (2×30 mL), and the combined organic layers were dried ($MgSO_4$) and concentrated to 5 mL. CH_2Cl_2 (30 mL) and Dess–Martin periodinane (0.85 g, 0.3 mmol, 15% solution in CH_2Cl_2) were added. The resulting colored solution was stirred for 1 h at 20°C, filtered through a plug (SiO_2; CH_2Cl_2), and concentrated to 50 mL. Malononitrile (14 mg, 0.21 mmol) and Al_2O_3 (50 mg, 0.49 mmol) were added, and the solution was heated to reflux for 1 h. Evaporation of the solvent and CC (SiO_2; CH_2Cl_2) afforded the desired products.

2-[7-(4-Dimethylaminophenyl)-5-(4-dimethylaminophenylethynyl)hepta-4-en-2,6-diynylidene]malononitrile (4b): The title compound was prepared from protected alcohol **17b** (100 mg, 0.21 mmol), following the general method. Dinitrile **4b** revealed to be unstable and, upon evaporation of the solvent, gave a black soot. Therefore the analytical characterization was carried out in CH_2Cl_2 solution. Yield 63 mg (≈70%). R_f= 0.72 (SiO_2; CH_2Cl_2); ^{1}H NMR (300 MHz, $CDCl_3$, 20°C, TMS): δ=3.02 (s, 6H; NCH_3), 3.03 (s, 6H; NCH_3), 6.25 (d, ^5J(H,H)=3.6 Hz, 1H; CH), 6.64 (d, ^3J(H,H)=9.0 Hz, 2H; Ar), 7.16 (d, ^5J(H,H)=3.6 Hz, 1H; CH), 7.41 (d, ^3J(H,H)=9.0 Hz, 2H; Ar), 7.46 ppm (d, ^3J(H,H)=9.0 Hz, 2H; Ar); ^{13}C NMR (75 MHz, $CDCl_3$, 20°C, TMS): δ=39.95, 86.29, 86.78, 88.33, 90.08, 96.86, 100.18, 103.18, 107.78, 111.48, 111.52, 111.67, 111.83, 113.27, 113.48, 115,97, 124.93, 133.64, 134.14, 139.89, 150.90, 150.95 ppm; UV/Vis (CH_2Cl_2): λ_{max} (ε)=300 (32000), 329 (sh, 33000), 534 nm (41000 mol^{-1} dm^3 cm^{-1}); HR-FT-MALDI-MS (3-HPA) *m/z*: calcd for $C_{28}H_{22}N_4^+$: 414.1839; found 414.1832 ([*M*]$^+$).

2-[9-(4-Dimethylaminophenyl)-7-(4-dimethylaminophenylethynyl)nona-6-en-2,4,8-triynylidene]malononitrile (5b): The title compound was prepared from alcohol **12** (100 mg, 0.25 mmol) following the general method for the oxidation and Knoevenagel condensation. Yield 97 mg (87%). Dark metallic solid. R_f=0.76 (SiO_2; CH_2Cl_2); M.p. >184°C (decomp); ^{1}H NMR (300 MHz, CD_2Cl_2, 20°C, TMS): δ=3.01 (s, 6H; NCH_3), 3.02 (s, 6H; NCH_3), 6.14 (d, ^7J(H,H)=1.5 Hz, 1H; CH), 6.65–6.70 (m, 4H; Ar), 7.11 (d, ^7J(H,H)=1.5 Hz, 1H; CH), 7.40 (d, J=9.0 Hz, 2H; Ar), 7.44 ppm (d, J=9.0 Hz, 2H; Ar); ^{13}C NMR (75 MHz, CD_2Cl_2, 20°C, TMS): δ=40.04, 80.02, 82.87, 86.72, 87.34, 95.29, 95.51, 98.72, 99.79, 101.99, 107.66, 107.73, 111.70, 111.81, 111.95, 112.77, 113.76, 124.87, 133.64, 133.95, 140.20, 151.30, 151.42 ppm; IR (neat): $\tilde{\nu}$=2853, 2163, 2125, 1599, 1520, 1355, 1165, 1102, 943, 811 cm^{-1}; UV/Vis (CH_2Cl_2): λ_{max} (ε)=293 (34500), 364 (25300), 530 nm (28500 mol^{-1} dm^3 cm^{-1}); HR-FT-MALDI-MS (3-HPA) *m/z*: calcd for $C_{30}H_{22}N_4^+$: 438.1839; found 438.1846 ([*M*]$^+$).

5-[Bis(4-dimethylaminophenyl)methylene]nona-1,8-dien-3,6-diyne-1,1,9,9-tetracarbonitrile (6a): The title compound was prepared from protected alcohol **18a** (50 mg, 0.083 mmol) following the general method

using twice the amount of nBu$_4$NF, Dess-Martin periodinane, and malononitrile. Yield 16 mg (42%), dark metallic solid. R_f=0.5 (SiO_2; CH_2Cl_2); m.p. 210–211 °C; ^{1}H NMR (300 MHz, CD_2Cl_2, 20 °C, TMS): δ= 3.10 (s, 12H; NCH_3), 6.69 (d, ^3J(H,H)=9.3 Hz, 4H; Ar), 7.07 (s, 2H; CH), 7.37 ppm (d, ^3J(H,H)=9.3 Hz, 4H; Ar); ^{13}C NMR (75 MHz, CD_2Cl_2, 20 °C, TMS): δ=40.33, 87.84. 89.61, 111.14, 112.45, 114.05, 120.76, 125.52, 134.94, 140.09, 153.96 ppm (2C missing); IR (neat): $\tilde{\nu}$= 2915, 2145, 2078, 1589, 1530, 1355, 1164, 941, 892, 819, 735 cm^{-1}; UV/Vis (CH_2Cl_2): λ_{max} (ε)=267 (17700), 313 (sh, 22200), 500 (49200), 632 nm (47400 mol^{-1} dm^3 cm^{-1}); HR-FT-MALDI-MS (3-HPA) m/z: calcd for $C_{30}H_{23}N_6^+$: 467.1979; found 467.1971 ([MH]$^+$).

5-[1,5-Bis(4-dimethylaminophenyl)penta-1,4-diyn-3-ylidene]nona-1,8-dien-3,6-diyne-1,1,9,9-tetracarbonitrile (6b): The title compound was prepared from protected alcohol **18b** (50 mg, 0.077 mmol) following the general method using twice the amount of nBu$_4$NF, Dess–Martin periodinane, and malononitrile. Yield 25 mg (64%), dark metallic solid. R_f=0.5 (SiO_2; CH_2Cl_2); M.p. >247 °C (decomp); ^{1}H NMR (300 MHz, CD_2Cl_2, 20 °C, TMS): δ=3.08 (s, 12H; NCH_3), 6.70 (d, ^3J(H,H)=9.3 Hz, 4H; Ar), 7.24 (s, 2H; CH), 7.51 ppm (d, ^3J(H,H)=9.3 Hz, 4H; Ar); ^{13}C NMR (75 MHz, CD_2Cl_2, 20 °C, TMS): δ=40.22, 91.44, 93.60, 106.83, 111.87, 111.99, 112.62, 130.76, 113.24, 135.33, 139.79, 152.20 ppm (3C missing); IR (neat): $\tilde{\nu}$=2904, 2115, 1591, 1526, 1422, 1360, 1155, 1112, 942, 811, 666 cm^{-1}; UV/Vis (CH_2Cl_2): λ_{max} (ε)=293 (31000), 320 (32700), 497 (28800), 629 nm (sh, 54300 mol^{-1} dm^3 cm^{-1}); HR-FT-MALDI-MS (3-HPA) m/z: calcd for $C_{34}H_{23}N_6^+$: 515.1979; found 515.1971 ([MH]$^+$).

Acknowledgements

This research was supported by the ETH Research Council and the Fonds der Chemischen Industrie (Germany). F. B. is indebted to the Ministry of Education, Youth, and Sport of the Czech Republic.

[1] For recent work, see: a) M. M. Oliva, J. Casado, M. M. M. Raposo, A. M. C. Fonseca, H. Hartmann, V. Hernandez, J. T. L. Navarrete, *J. Org. Chem.* **2006**, *71*, 7509–7520; b) A. J. Zucchero, J. N. Wilson, U. H. F. Bunz, *J. Am. Chem. Soc.* **2006**, *128*, 11872–11881; c) H. Meier, B. Mühling, A. Oehlhof, S. Theisinger, E. Kirsten, *Eur. J. Org. Chem.* **2006**, 405–413; d) J. C. Collings, A. C. Parsons, L-Porrès, A. Beeby, A. S. Batsanov, J. A. K. Howard, D. P. Lydon, P. J. Low, I. J. S. Fairlamb, T. B. Marder, *Chem. Commun.* **2005**, 2666–2668; e) H. Meier, J. Gerold, H. Kolshorn, B. Mühling, *Chem. Eur. J.* **2004**, *10*, 360–370; f) A. S. Andersson, K. Qvortrup, E. R. Torbensen, J.-P. Mayer, J.-P. Gisselbrecht, C. Boudon, M. Gross, A. Kadziola, K. Kilsa, M. B. Nielsen, *Eur. J. Org. Chem.* **2005**, 3660–3671.

[2] For recent investigations on nonlinear optical effects in push–pull chromophores, see: a) N. K. Pahadi, D. H. Camacho, I. Nakamura, Y. Yamamoto, *J. Org. Chem.* **2006**, *71*, 1152–1155; b) G. Archetti, A. Abbotto, R. Wortmann, *Chem. Eur. J.* **2006**, *12*, 7151–7160; c) S. R. Marder, *Chem. Commun.* **2006**, 131–134; d) S. Kato, T. Matsumoto, M. Shigeiwa, H. Gorohmaru, S. Maeda, T. Ishi-i, S. Mataka, *Chem. Eur. J.* **2006**, *12*, 2303–2317; e) V. Kriegisch, C. Lambert, *Eur. J. Inorg. Chem.* **2005**, 4509–4515; f) D. Locatelli, S. Quici, D. Roberto, F. De Angelis, *Chem. Commun.* **2005**, 5405–5407; g) K. Koynov, A. Bahtiar, C. Bubeck, B. Mühling, H. Meier, *J. Phys. Chem. B* **2005**, *109*, 10184–10188; h) E. Zojer, D. Beljonne, P. Pacher, J.-L. Brédas, *Chem. Eur. J.* **2004**, *10*, 2668–2680; i) S. Kato, T. Matsumoto, T. Ishi-i, T. Thiemann, M. Shigeiwa, H. Gorohmaru, S. Maeda, Y. Yamashita, S. Mataka, *Chem. Commun.* **2004**, 2342–2343.

[3] a) R. R. Tykwinski, U. Gubler, R. E. Martin, F. Diederich, C. Bosshard, P. Günter, *J. Phys. Chem. A* **1998**, *102*, 4451–4465; b) U. Gubler, R. Spreiter, C. Bosshard, P. Günter, R. R. Tykwinski, F. Diederich, *Appl. Phys. Lett.* **1990**, *73*, 2396–2398.

[4] a) J. C. May, J. H. Lim, I. Biaggio, N. N. P. Moonen, T. Michinobu, F. Diederich, *Opt. Lett.* **2005**, *30*, 3057–3059; b) N. N. P. Moonen, W. C. Pomerantz, R. Gist, C. Boudon, J.-P. Gisselbrecht, T. Kawai, A. Kishioka, M. Gross, M. Irie, F. Diederich, *Chem. Eur. J.* **2005**, *11*, 3325–3341; c) G. Jiang, T. Michinobu, W. Yuan, M. Feng, Y. Wen, S. Du, H. Gao, L. Jiang, F. Diederich, D. Zhu, *Adv. Mater.* **2005**, *17*, 2170–2173; d) N. N. P. Moonen, F. Diederich, *Org. Biomol. Chem.* **2004**, *2*, 2263–2266; e) N. N. P. Moonen, R. Gist, C. Boudon, J.-P. Gisselbrecht, P. Seiler, T. Kawai, A. Kishioka, M. Gross, M. Irie, F. Diederich, *Org. Biomol. Chem.* **2003**, *1*, 2032–2034.

[5] a) T. Michinobu, C. Boudon, J.-P. Gisselbrecht, P. Seiler, B. Frank, N. N. P. Moonen, M. Gross, F. Diederich, *Chem. Eur. J.* **2006**, *12*, 1889–1905; b) T. Michinobu, J. C. May, J. H. Lim, C. Boudon, J.-P. Gisselbrecht, P. Seiler, M. Gross, I. Biaggio, F. Diederich, *Chem. Commun.* **2005**, 737–739.

[6] B. Feith, H.-M. Weber, G. Maas, *Chem. Ber.* **1986**, *119*, 3276–3296.

[7] D. L. Boger, R. J. Wisocki, *J. Org. Chem.* **1988**, *53*, 3408–3421.

[8] a) K. A. Leonard, M. I. Nelen, T. P. Simard, S. R. Davies, S. O. Gollnick, A. R. Oseroff, S. L. Gibson, R. Hilf, L. B. Chen, M. R. Detty, *J. Med. Chem.* **1999**, *42*, 3953–3964; b) K. A. Leonard, M. I. Nelen, L. T. Anderson, S. L. Gibson, R. Hilf, M. R. Detty, *J. Med. Chem.* **1999**, *42*, 3942–3952; c) A. Auffrant, F. Diederich, C. Boudon, J.-P. Gisselbrecht, M. Gross, *Helv. Chim. Acta* **2004**, *87*, 3085–3105.

[9] S. Mann, S. Carillon, O. Breyne, A. Marquet, *Chem. Eur. J.* **2002**, *8*, 439–450.

[10] Y. Rubin, S. S. Lin, C. B. Knobler, J. Anthony, A. M. Boldi, F. Diederich, *J. Am. Chem. Soc.* **1991**, *113*, 6943–6949.

[11] M. Bellassoued, A. Majidi, *J. Org. Chem.* **1993**, *58*, 2517–2522.

[12] J. Anthony, A. M. Boldi, Y. Rubin, M. Hobi, V. Gramlich, C. B. Knobler, P. Seiler, F. Diederich, *Helv. Chim. Acta* **1995**, *78*, 13–45.

[13] E. J. Corey, P. L. Fuchs, *Tetrahedron Lett.* **1972**, *36*, 3769–3772.

[14] A. Bauer, M. W. Miller, S. F. Vice, S. W. McCombie, *Synlett* **2001**, *2*, 254–256.

[15] Y. Kobayashi, M. Ito, *Eur. J. Org. Chem.* **2000**, *20*, 3393–3397.

[16] a) M. Fitzegerald, J. H. Bowie, S. Dua, *Org. Biomol. Chem.* **2003**, *1*, 1769–1778; b) M. Ishikawa, Y. Hasegava, A. Kunai, T. Yamanaka, *J. Organomet. Chem.* **1990**, *381*, C57–C59; c) V. Fiandanese, D. Bottalico, G. Marchese, A. Punzi, *Tetrahedron* **2004**, *60*, 11421–11425.

[17] M. Journet, D. Cai, L. M. DiMichele, L. D. Larsen, *Tetrahedron Lett.* **1998**, *39*, 6427–6428.

[18] a) D. B. Dess, J. C. Martin, *J. Org. Chem.* **1983**, *48*, 4155–4156; b) R. Suzuki, H. Tsukuda, N. Watanabe, Y. Kuwatani, I. Ueda, *Tetrahedron* **1998**, *54*, 2477–2496.

[19] W. P. Griffith, S. V. Ley, *Aldrichimica Acta* **1990**, *23*, 13–19.

[20] A. J. Mancuso, S.-L. Huang, D. Swern, *J. Org. Chem.* **1987**, *52*, 2480–2482.

[21] G. Klebe, *Struct. Chem.* **1990**, *1*, 597–616.

[22] C. Dehu, F. Meyers, J. L. Brédas, *J. Am. Chem. Soc.* **1993**, *115*, 6198–6206.

[23] J.-P. Gisselbrecht, N. N. P. Moonen, C. Boudon, M. B. Nielsen, F. Diederich, M. Gross, *Eur. J. Org. Chem.* **2004**, 2959–2972.

[24] a) M. G. Kuzyk, *Opt. Lett.* **2000**, *25*, 1183–1185; b) M. G. Kuzyk, *Opt. Lett.* **2003**, *28*, 135.

[25] Y. Araki, T. Konoike, *J. Org. Chem.* **1997**, *62*, 5299–5309.

Received: December 4, 2006
Published online: February 16, 2007

